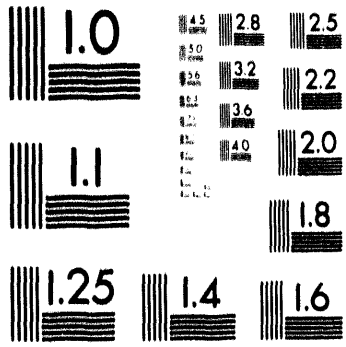
1.0
1.1
1.25
1.4
1.6
1.8
2.0
2.2
2.5
2.8
3.2
3.6
4.0
4.5
5.0

1 of 1

SAND92-1986
Unlimited Release

Category UC-25

Improvement of the Stability of the Process for Synthesizing Chemically Prepared Varistor Powder

S. J. Lockwood
Ceramic and Glass Processing Department

E. V. Thomas
Statistics and Human Factors Department

Sandia National Laboratories
Albuquerque, NM 87185

Abstract

High field varistors are utilized as voltage regulators in neutron generators. Varistor material is currently supplied by a single, proprietary commercial source. The chem-prep varistor process was developed as a backup/replacement for that source. With the transfer of the chem-prep process from the development lab to the production facility, studies were initiated to verify that the process was stable in the manufacturing environment (i.e., robust with respect to variation inherent in the process). Earlier studies had identified the key processing variables as the two precipitants, oxalic acid and sodium hydroxide, and the major metal species, zinc chloride.

To evaluate the chem-prep process stability we considered two issues. First, we needed quantitative information concerning the magnitude of the uncertainty associated with assaying the three major precursors; oxalic acid, sodium hydroxide, and zinc chloride. Second, we needed to understand how variations in composition as a result of assay variability affected the physical/electrical properties of the varistors. Process stability was then determined by comparing the assay uncertainty region with the precipitant/$ZnCl_2$ compositional region meeting electrical and physical property specifications.

Assay variability, both within and among laboratories, was assessed by conducting a round robin among the analytical laboratories at SNL and the production facilities. The round robin study demonstrated that the standard deviations of repeated assays of the same sample (for the three analytes) by the same labs were about 0.1 wt%. Systematic assay differences among laboratories were typically in the range from 0.1 - 0.4 wt%. This information was used to help design a second study.

In the second study, a mixture experiment was conducted to make an assessment of the effects of the precipitants/$ZnCl_2$ on the breakdown field (E), the nonlinearity coefficient (α), and the bulk density. Based on the experimental data, models of these three properties were constructed. From the models the precipitant/$ZnCl_2$ compositional region meeting electrical and physical property specifications was identified.

From these two studies we have concluded that the chem-prep process can be stable over a wide precipitant/$ZnCl_2$ region. However, we found that the nominal target composition is on the edge of this region and that slight variations in the precipitant/$ZnCl_2$ composition from the nominal target resulted in varistor material that did not meet electrical and physical property specifications. Thus, in an effort to make the process stable with respect to assay variability, the nominal composition was moved to the center of that relatively large region with acceptable electrical and physical properties. Tests of unpotted component rods made from the new precipitant/$ZnCl_2$ composition met all electrical and physical property specifications and performed similarly to rods fabricated from the original target composition.

Acknowledgements:

The authors gratefully acknowledge the major contribution of Sally Douglas in preparing all of the chem-prep batches used in this study. The authors also acknowledge the efforts of the many personnel in the analytical labs at ATI, MMSC, and SNL (Departments 1824 and 2472). And finally, it should not be forgotten that all work on the high field varistor program builds upon the tremendous teamwork and previous accomplishments of the V-Team.

Table of Contents

List of Tables

List of Figures

I. Introduction:

High field varistors are used as voltage regulators in neutron generators. Varistors function as electrical insulators (resistors) at low voltages, but become electrically conducting at or above a certain voltage known as the breakdown voltage. At voltages above this breakdown value, varistors exhibit nonlinear current-voltage behavior, described by the following equation:

$$I = KV^{\alpha}$$

where I is the current, K is a constant, V is the voltage, and α is the nonlinearity coefficient. The nonlinearity coefficient is the reciprocal of the slope of the I-V curve in the nonlinear region and is therefore a measure of the sharpness of the transition from resistor to conductor.

All varistors to date have been supplied by a single, proprietary source. Although these varistors have satisfactorily met product specifications and production requirements, there has been a concern about the vulnerability of depending on a single source that has only a very limited number of people fully knowledgeable in that processing technology. In the early 1980's a program was initiated by Department 2565 to develop a second varistor source. A chemical preparation process for making homogenous, high purity zinc oxide-based varistor powder was developed by Departments 1846 and 2476. Additional development work by Department 2476 generated the ceramic forming, sintering, and machining procedures needed for fabrication of the chem-prep material into the varistor component (rod).

Many of the chemical preparation processing conditions were set during the initial laboratory-scale development work by Dosch and Kimball.[1] However, during the scale-up phase of the project a number of processing variables were studied and changed in response to meeting component specifications. The required doping of Al^{3+} and Na^{+}, the detrimental effects of Cl^{-}, and the effects of sample geometry and sintering schedule on electrical and physical properties were investigated.[2-5] By the end of 1989 a reproducible, production-scale process had been developed at SNL that would generate varistors meeting all component electrical and physical property specifications. Evaluation of the chem-prep varistor components at the neutron generator sub-assembly level was completed in 1991.

With the transfer of the chem-prep technology to two potential suppliers, Alliant Techsystems, Inc. (ATI, formerly Honeywell, Inc.) and Martin Marietta Specialty Components (MMSC, formerly General Electric Neutron Devices Department), establishment or verification of production process control needed to be addressed. Based on empirical data, primarily from SNL, the process appeared to be stable. However, a reproducible process performed by a single operator in a development lab does not necessarily translate into a stable/robust process in a production environment.

Solution chemistry is the key to process stability. The pH and the kinetics of the reactions determines the completeness and homogeneity of the precipitates. The key process controlling factors are the concentrations of the precipitants, sodium hydroxide [NaOH] and oxalic acid [$H_2C_2O_4$]), and the major metal species, zinc chloride ($ZnCl_2$). Hereafter, the concentrations of these three factors taken together will be referred to as a composition even though the interaction of the three involves a two-step process. The concentration of each factor was determined by titermetric assay.

A five lab round robin was conducted to assess assay variation both within and among labs. A statistically designed experiment in which the concentrations of the three compositional factors, NaOH, $H_2C_2O_4$, $ZnCl_2$, were systematically varied was performed. The remaining process variables (i.e., $CoCl_2$, $MnCl_2$, $AlCl_3$, and $Na_2C_2O_4$) were held constant. The electrical and physical properties of varistors fabricated from the powders generated by the experiment were modelled and used to define the region(s) where acceptable product could be generated. As a result, an evaluation was made of a new composition that was predicted by the models to be more robust with respect to compositional variation due to assaying errors. Finally, analyses of batches from compositions that failed to meet one or more specifications were conducted with the aim to increase our understanding of solution chemistry-materials properties relationships.

II. Procedures:

A. Round Robin

Five labs participated in the assay round robin. Three of the labs were from SNL: the 1824 Analytical Lab, the 2472 Analytical Lab, and the 2476 Ceramics Lab. The other participants were the analytical labs from ATI and MMSC. The four analytical labs were given four coded samples each of the $ZnCl_2$, $H_2C_2O_4$, and NaOH. For the $ZnCl_2$ and $H_2C_2O_4$, the four samples represented three different lots of material, with two of the samples from the same lot. For the NaOH only one lot was available, so four coded samples from the single lot were supplied for analysis. Each lab followed the assay procedures described in SS393278 (Assaying Procedures for Precipitants (NaOH, $H_2C_2O_4 \cdot 2H_2O$) and SS393277 (Assaying Procedures for Salt Precursor Stock Solutions). Each lab submitted triplicate analyses of each sample. Along with results obtained by the 2476 Ceramics Lab (the results from this lab were not strictly part of the round robin procedure [i.e., the 2476 analyzed samples were not coded or blind]) these data were used to construct a statistical model which was used to describe the observed variability of the assay values.

The statistical model used to describe the variation in the assay results is

$$Y_{ijk} = \alpha_i + \beta_j + \gamma_{ij} + \varepsilon_{ijk}, \text{ where}$$

Y_{ijk} is the reported analyte value of the k^{th} replicate done by the j^{th} lab on the i^{th} sample, α_i is the true (but unknown) value of the analyte in the i^{th} sample, β_j is the systematic bias of

the j^{th} lab (subject to a side condition like $\beta_1=0$), γ_{ij} is the specific effect of the j^{th} lab on the i^{th} sample, and ε_{ijk} is the random measurement error associated with the k^{th} replicate by the j^{th} lab on the i^{th} sample. Note that the true values of the analytes are assumed to be random.

The random measurement errors, ε_{ijk} are assumed to be independent with mean zero and variance, $\sigma^2_{\varepsilon_j}$. The magnitude of $\sigma^2_{\varepsilon_j}$ is reflective of the ability of the j^{th} lab to repeat the assay on the sample (repeatability). By incorporating the subscript j in σ^2_{ε}, this model is generalized to allow for lab-specific errors of repeatability. By virtue of the assumed randomness of the α_i terms, the γ_{ij} terms are random with zero mean and variance σ^2_γ. The magnitude of σ^2_γ is a measure of the consistency of the systematic effects of the different laboratories. Note that because we do not know α_i we cannot say anything about the accuracy of the assays in an absolute sense. Nevertheless, we can compare assays across laboratories. To assess the statistical significance of differences between labs (e.g., $\beta_2-\beta_1$), we estimated $\sigma^2_{\varepsilon_j}$ and σ^2_γ.

B. Powder Synthesis and Wafer Fabrication

Chem-prep powder was prepared following SS392386 (Batch-Type Powder Preparation by the Sodium-Doped Chloride Process) with the exception of compositional modifications for the mixture design described below. Two 60g wafers were fabricated from each powder composition and sintered at 725°C for 16h according to SS392387 (Wafer Fabrication). Breakdown field (E), nonlinearity coefficient (α), bulk density, and % open porosity were measured for the wafers following the appropriate SS drawing (reference to the specific document is classified CRD). The data were then modelled to estimate the effect of composition on those properties. A schematic of the chem-prep process along with the nominal composition and electrical and physical property specifications is shown in Figure 1.

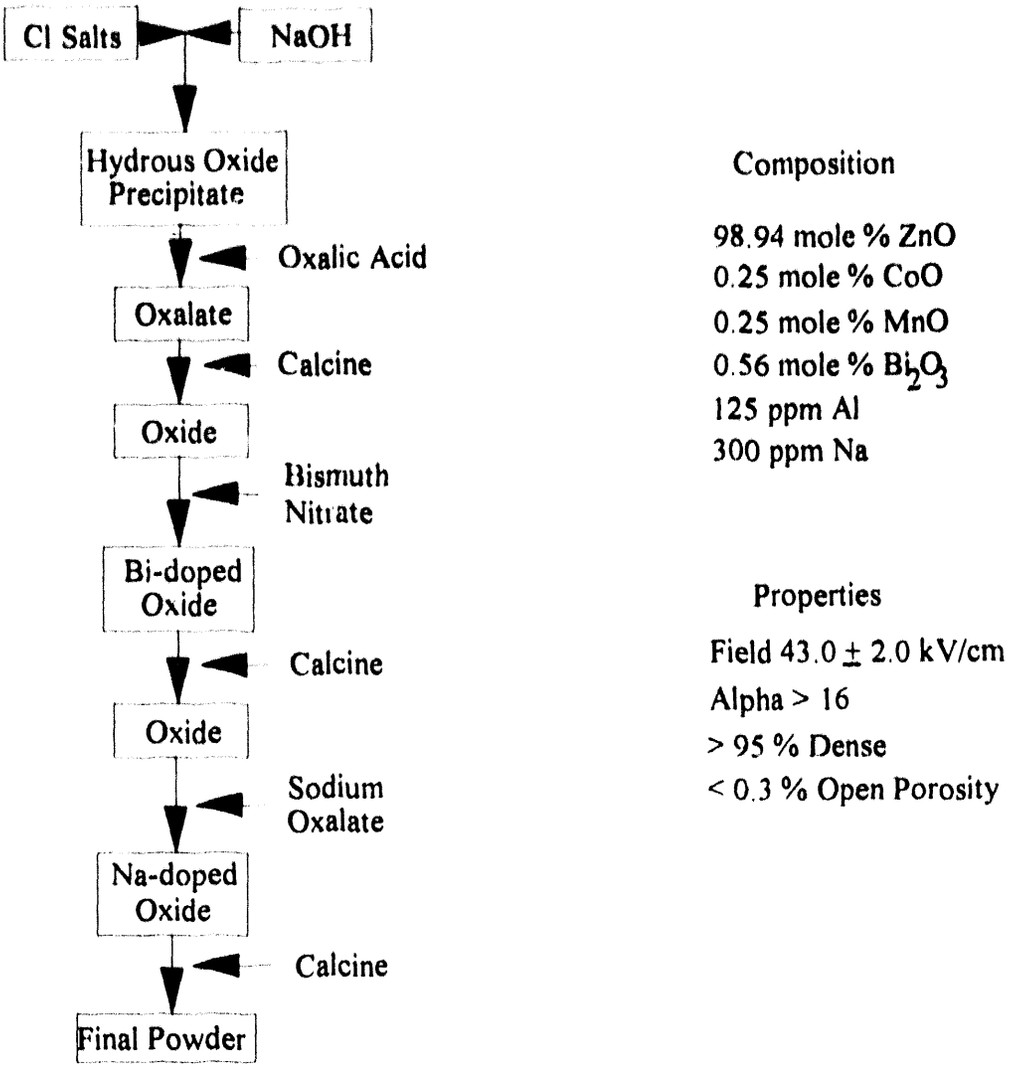

Figure 1. The Varistor Chem-prep Process

C. Mixture Design

The key processing variables in the chem-prep process are the two precipitants, $H_2C_2O_4$ and NaOH, and the major metal species, $ZnCl_2$. These three major components control the pH and therefore determine the overall solution chemistry. The steps involving the three components can be described by the following two step process:

$$ZnCl_2 + 2NaOH \rightarrow Zn(OH)_2 + 2NaCl$$
$$Zn(OH)_2 + H_2C_2O_4 \rightarrow ZnC_2O_4 + 2H_2O$$

If the amounts of the minor components (i.e., Bi, Co, Mn, Al, and Na) are held constant, the three major components can be viewed as a ternary mixture. However, only a small portion

of the full ternary diagram is of interest. Compositions (i.e, ratios of the three components) that significantly deviate from chemical stoichiometry will not result in acceptable product. The ideal design will encompass the largest range of compositions providing measurable data that can be modelled. Based on empirical data and processing experience, relationships between two or more of the components can be limited by defining a series of constraints. These design constraints, listed in Table 1, are based on two factors. One is to ensure that the compositional variation in the design exceeds the variation in composition due to errors in assaying the starting materials. The round robin evaluation (see the Results and Discussion section) was performed to assess the magnitude of the assaying errors. The weight percent ranges indicated in Table 1 are at least several times larger than the assay errors as determined by the round robin evaluation. Greater deviations from stoichiometry would result in significant wastage of one or more components due to nonreaction and would require more careful processing to ensure complete removal of the excess component. The second factor influencing the design constraints was based on previous work that had shown that it was necessary to drive the reaction to a basic pH to ensure complete precipitation of all metal species. Therefore, the design constraints favor NaOH excess compositions.

Table 1. Mixture Design Constraints

$ZnCl_2$ limits	$\pm$ 3 wt% of nominal and $\leq 1.03 \times [H_2C_2O_4]$
$H_2C_2O_4$ limits	$\pm$ 3 wt% of nominal
NaOH limits	$\geq 2.00 \times [ZnCl_2]$ and $> 2.00 \times [H_2C_2O_4]$

Figure 2 shows the ternary diagram with the design constraint vectors. The shaded portion of the diagram defines the compositional area to be investigated and modelled. The nominal composition is identified with an asterisk. Outlining the nominal composition is the region of compositional variation from the target due to assaying uncertainty (see the discussion of the Round Robin).

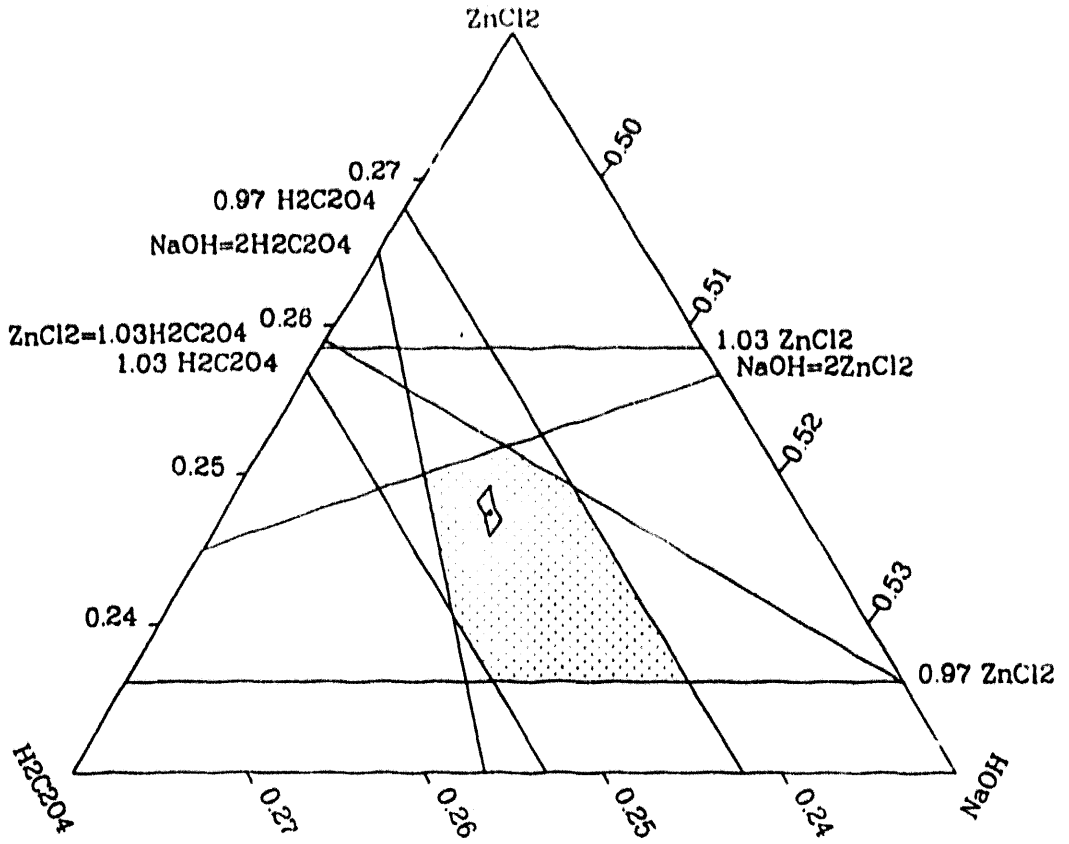

Figure 2. Compositional Ternary Diagram with Design Constraints

An experiment involving eight unique compositions, well spread out and spanning the region of interest, was performed. These eight compositions, usually at the intersection of constraint lines with respect to two of the components, are displayed in Figure 3. These eight compositions (with a replicate at the center point composition [8]) were generated in a randomized order. Table 2 lists the compositions by mole fraction, the run order and includes an entry that shows the assay "error" that would be required to generate that composition if the nominal composition had been the target. Composition 1 is the stoichiometric composition. The nominal composition has 2 mole % excess NaOH.

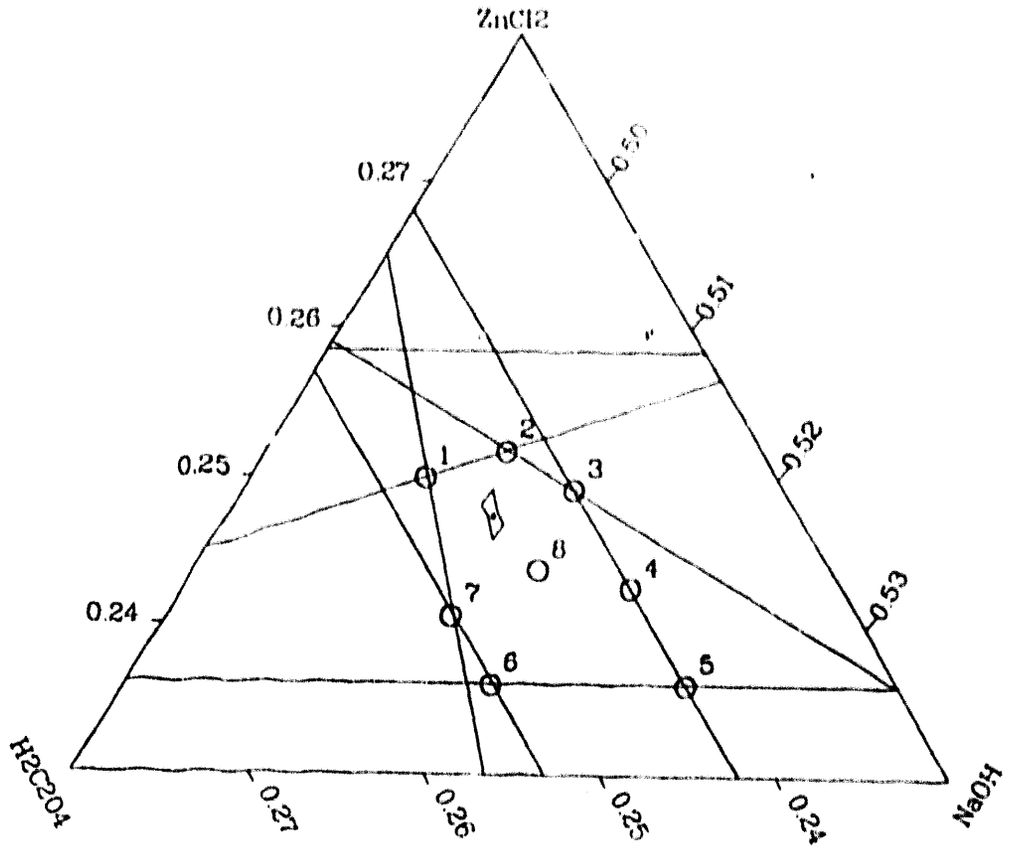

Figure 3. Mixture Design

Table 2. Mixture Design Composition and Run Order

		Zinc Chloride		Oxalic Acid		Sodium Hydroxide	
Comp. #	Run #	Mole Fraction	Assay "Error" (wt%)	Mole Fraction	Assay "Error" (wt%)	Mole Fraction	Assay "Error" (wt%)
1	2	0.2500	-0.46	0.2500	-1.01	0.5000	0.49
2	4	0.2518	-0.78	0.2445	1.21	0.5037	0.13
3	6	0.2492	-0.31	0.2419	2.26	0.5089	-0.39
4	3	0.2426	0.90	0.2419	2.26	0.5155	-1.04
5	7	0.2361	2.08	0.2419	2.26	0.5220	-1.68
6	5	0.2361	2.08	0.2531	-2.26	0.5108	-0.58
7	8	0.2407	1.24	0.2531	-2.26	0.5062	-0.12
8	1,9	0.2438	0.68	0.2466	0.37	0.5096	-0.46

During the oxalate precipitation step, at 60 min intervals following the oxalic acid addition, 20 ml slurry samples were taken from the reaction vessel at the top, middle, and bottom. The reactions were quenched with methanol and then washed with methanol and filtered to obtain a dry oxalate sample. These samples were analyzed for bulk elemental composition (following SS392386 and SS393279 [Composition and Trace Analyses by ICP-AES]) and used to correlate mixing time and oxalate slurry homogeneity effects with the electrical and physical property models.

It was anticipated that one or more of the compositions would have insufficient base excess to reach the Process Specification requirement of pH 8.0 within 150 min. Instead of discarding the batches as called for in SS392386, those batches were terminated at 180 min regardless of the pH and processing of the batches was completed through wafer testing.

The electrical properties, breakdown field and nonlinearity coefficient, and the physical characteristic, bulk density, were measured from wafers prepared from each composition. Taken together, these measurements enabled an assessment of the sensitivity of these properties to compositional variation. Low-order polynomial models (up to quadratic) for each of these properties (in terms of the mole fractions of the three starting materials: $ZnCl_2$, $H_2C_2O_4$, and NaOH) were developed to summarize the effects of compositional variation on each electrical/physical property. Specifically, these models are of the form,

$Y = \beta_0 + \beta_1 \cdot X_1 + \beta_2 \cdot X_2 + \beta_{11} \cdot X_1^2 + \beta_{22} \cdot X_2^2 + \beta_{12} \cdot X_1 \cdot X_2 + \varepsilon$, where

Y is the observed property,

$$X_1 = \log_e\left(\frac{\text{mole fraction of } ZnCl_2}{\text{mole fraction of NaOH}}\right),$$

$$X_2 = \log_e\left(\frac{\text{mole fraction of } H_2C_2O_4}{\text{mole fraction of NaOH}}\right),$$

ε is a measurement error, and the $\beta_{i(j)}$'s are parameters to be estimated. In conjunction with the round robin results, these models were used to assess the effects of assay errors on these properties.

III. Results and Discussion:

A. Round Robin

The initial examination of the analytical results from the round robin study indicated some very significant lab-to-lab differences. However, the largest deviations were attributed to procedural errors, a sample packaging error, and one spreadsheet calculation error. All but the packaging error were subsequently corrected (time considerations did not allow for the samples packaged incorrectly to be repeated) and analysis of those corrected results are presented in the remainder of this section. Results from the 2476 Ceramics Lab are included although the analysis performed in that lab was not performed on coded or blind samples. In

the case of the duplicate samples from the same lot only the single 2476 Ceramics Lab analysis was compared to the other analytical results.

With respect to the $ZnCl_2$ assays, there are a number of interesting differences among the laboratories. Summaries of the statistical analysis are presented in Tables 3 and 4. The metric presented in Table 3, $\hat{\sigma}_{\varepsilon_j}$, is reflective of the ability of each laboratory to repeat an assay on the same sample. In fact, $\hat{\sigma}_{\varepsilon_j}$ is the estimate of the standard deviation of these repeated assays (see the Appendix for the computational method used to obtain the $\hat{\sigma}_{\varepsilon_j}$). These repeated assays involved separate sample preparations and titrations. Therefore, the metrics displayed are with regard to the ability to repeat not only the titration, but also the sample preparation. By assuming that the random measurement errors, ε_{ijk}, are normally distributed, the ordering of the laboratories with respect to $\hat{\sigma}_{\varepsilon_j}$ was determined to be: {ATI}<{1824, MMSC}<{2476, 2472}. That is, the repeatability of ATI is superior to that of 1824 and MMSC, which in turn are superior to that of 2476 and 2472. Note that the repeatabilities of 1824 and MMSC are statistically indistinguishable, as are the repeatabilities of 2476 and 2472.

Table 3. Estimated Errors of Repeatability for $ZnCl_2$ Assays, by Laboratory (j)

	2476 (j=1)	2472 (j=2)	1824 (j=3)	ATI (j=4)	MMSC (j=5)
$\hat{\sigma}_{\varepsilon_j}$	0.12	0.13	0.047	0.021	0.066

Now we consider systematic differences across laboratories. Figure 4 displays the average $ZnCl_2$ assay per sample for each laboratory. Table 4 summarizes the systematic differences among the laboratories. As mentioned previously in the discussion of the statistical model, only the differences among the β_j's can be compared, as the β_j's cannot be directly estimated. To generate these comparisons, 2476 (j = 1) will be used as the reference point to estimate systematic differences between 2476 and the other laboratories.

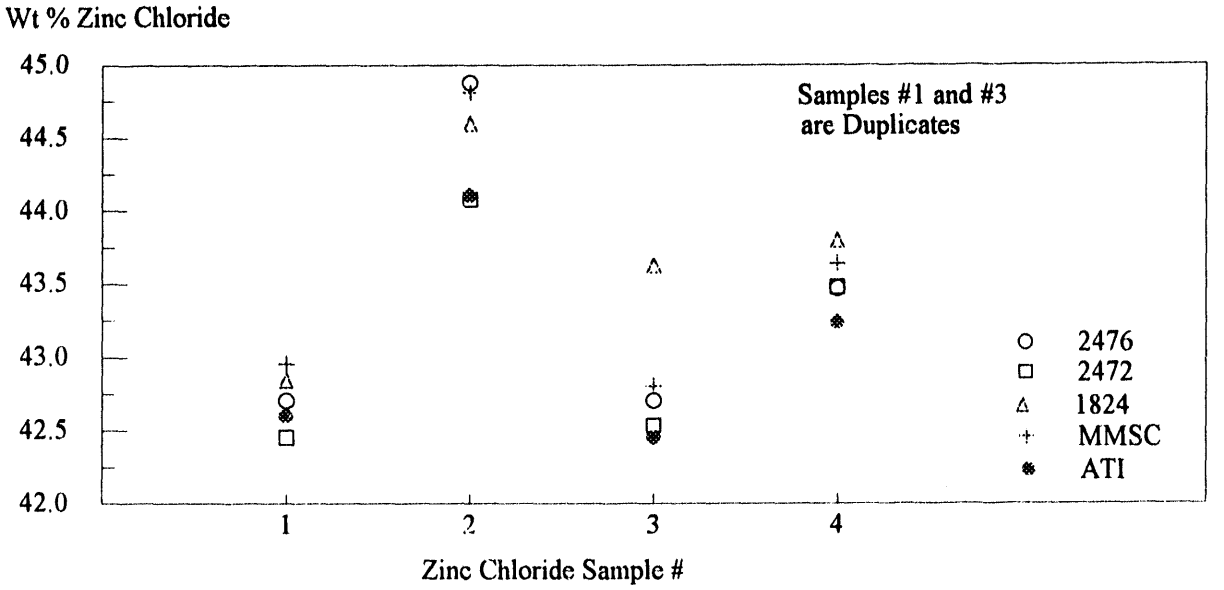

Figure 4. Analytical Round Robin - Zinc Chloride Assay

Table 4 contains estimates of these contrasts given by $C_j = \beta_j - \beta_1$. To assess the statistical significance of these contrasts, we need estimates of σ_γ as well as the various σ_{ε_j}'s. Table 3 provides the latter, while using the methods in the Appendix, we find that $\hat{\sigma}_\gamma = 0.24$. Notice that $\hat{\sigma}_\gamma$ is large relative to the various σ_{ε_j}'s and comparable in magnitude to the various $\hat{C}_j$'s. This indicates that the magnitude of the differences among the laboratories is inconsistent from sample to sample. Nevertheless, we can (again assuming normality and using the methods discussed in the Appendix) show that there are some statistically distinguishable systematic differences among the laboratories. These can be represented by:

ATI 2472 2476 MMSC 1824

This display orders the different laboratories from low to high with respect to the average $ZnCl_2$ assay across all four samples. A line connects those laboratories that are statistically indistinguishable. For instance, $ZnCl_2$ assays performed at ATI produced statistically lower values than $ZnCl_2$ assays from all of the other laboratories, except 2472.

Table 4. Systematic Differences Among the Laboratories (wt% $ZnCl_2$)

	2476 (j=1)	2472 (j=2)	1824 (j=3)	ATI (j=4)	MMSC (j=5)
$\hat{C}_j$	----	-0.31	0.28	-0.34	0.12

It is not possible to use the round robin results to make an assessment of the accuracy of an individual laboratory's assays for $ZnCl_2$ since an absolute reference was not available. However, it is possible to use the round robin results to provide a model that can be used to describe the variation between assays from two different laboratories. For example, suppose that a sample was submitted to 1824 and ATI (the laboratories providing the most discrepant results for $ZnCl_2$) for analysis and that each laboratory was to perform n independent assays of that sample. Using the measurement model we have developed, the difference between the averages of the $ZnCl_2$ assays between the two laboratories, $\overline{Y}_{1824}$ - $\overline{Y}_{ATI}$, is approximately normal with an average of about 0.62 wt% and a standard deviation of about $\sqrt{\frac{(\hat{\sigma}^2_{\varepsilon_3} + \hat{\sigma}^2_{\varepsilon_4})}{n} + 2 \cdot \hat{\sigma}^2_{\gamma}}$. In this case, because $\hat{\sigma}^2_{\varepsilon_3}$ and $\hat{\sigma}^2_{\varepsilon_4}$ are so small compared to $\hat{\sigma}^2_{\gamma}$, the value of n has little effect on the estimated standard deviation which is about 0.34. This provides a feel for the magnitude of interlaboratory differences that we might expect (about one wt%).

With regard to the $H_2C_2O_4$ assays, the analysis is somewhat simpler than that of the $ZnCl_2$ assays. This is due to the fact that the ability to repeat $H_2C_2O_4$ assays is consistent across laboratories (see Table 5). The combined estimate of σ_ε is $\hat{\sigma}_\varepsilon = 0.12$.

Table 5. Estimated Std. Dev. of Repeated Measurements (wt%) for $H_2C_2O_4$ Assays

	2476 (j=1)	2472 (j=2)	1824 (j=3)	ATI (j=4)	MMSC (j=5)
$\hat{\sigma}_{\varepsilon_j}$	0.13	0.10	0.12	0.09	0.14

There are however, some interesting systematic differences among the laboratories. Figure 5 displays the average $H_2C_2O_4$ assay per sample for each laboratory. Table 6 summarizes the systematic differences among the laboratories observed in Figure 5.

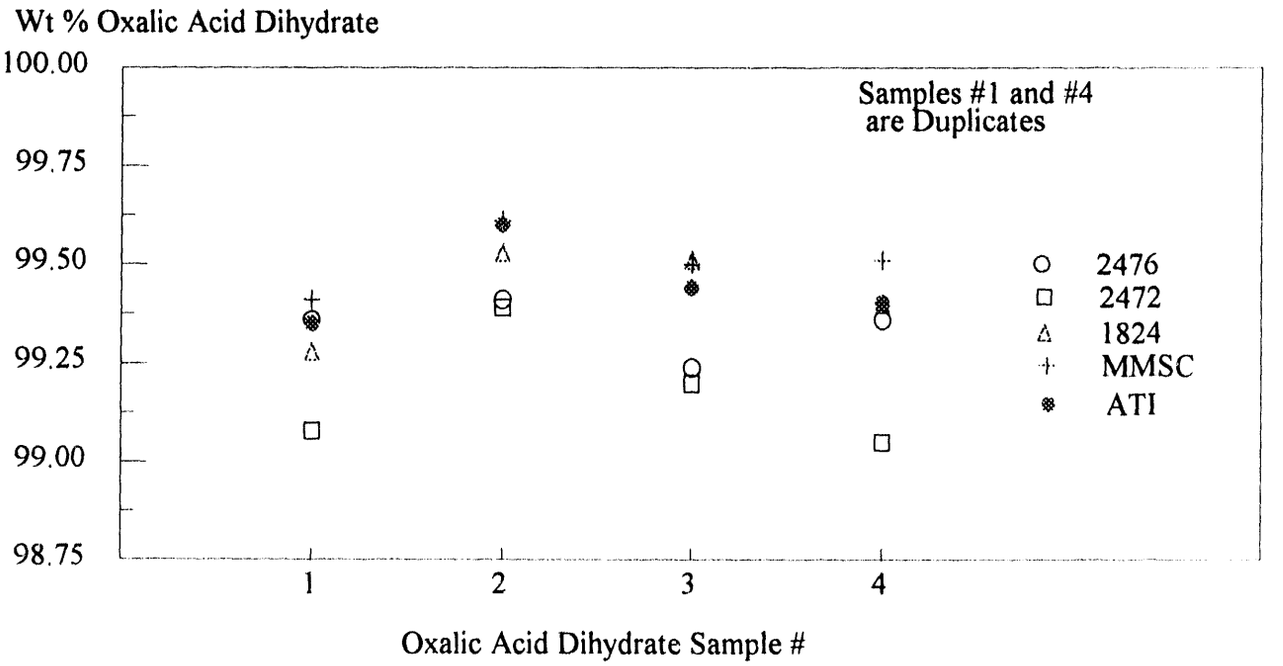

Figure 5. Analytical Round Robin - Oxalic Acid Assay

Again, we will use 2476 (j = 1)as the reference point to compare the estimates of the systematic differences among the laboratories. Table 6 contains estimates of these differences ($C_j = \beta_j - \beta_1$). To assess the statistical significance of these differences we use the methods in the Appendix with $\hat{\sigma}_\gamma = 0.039$ and $\hat{\sigma}_\varepsilon = 0.12$. Notice that $\hat{\sigma}_\gamma$ is somewhat smaller in magnitude than the various $\hat{C}_j$'s, indicating that the systematic differences among the laboratories are relatively consistent from sample to sample.

Table 6. Systematic Differences Among the Laboratories (wt% $H_2C_2O_4$)

	2476 (j=1)	2472 (j=2)	1824 (j=3)	ATI (j=4)	MMSC (j=5)
$\hat{C}_j$	----	-0.13	0.09	0.11	0.17

Again, assuming normality and using the methods discussed in the Appendix, we can distinguish systematic differences among the laboratories. These can be represented by:

2472 2476 1824 ATI MMSC

Here, the important distinction among the laboratories is that 2472 appears to be different from the rest. Suppose that a sample was submitted to 2472 and MMSC (the laboratories providing the most discrepant results for $H_2C_2O_4$) for analysis and that each laboratory was to perform n independent assays of that sample. Using the measurement model, the difference between the averages of the $H_2C_2O_4$ assays between the two laboratories, $\overline{Y}_{2472}$ - $\overline{Y}_{ATI}$, is approximately normally distributed with an average of about 0.30 wt% and a standard deviation of about $\sqrt{2\cdot(\frac{\hat{\sigma}_\varepsilon^2}{n}+\hat{\sigma}_\gamma^2)}$ (0.18 for n=1). Thus, even with the statistical uniqueness of 2472, it is unlikely that differences of individual $H_2C_2O_4$ assays (i.e., n=1) among these five laboratories will exceed one-half to one weight percent.

Assays of the third component, NaOH, differed from the previous two in that only a single lot of material was available. However, four coded samples from the single lot were still submitted to be analyzed in triplicate by four of the five laboratories (2476 analyzed only one sample in triplicate). For purposes of analysis, we will regard the coded samples as different. Also, from Figure 6 which displays the average NaOH assay per sample for each laboratory, it can be seen that the results for MMSC were markedly lower than the others. This was due to a packaging error in the shipping containers and resulted in the NaOH reacting with the packing cap material. Therefore, in the statistical analysis that follows, the MMSC results were not considered.

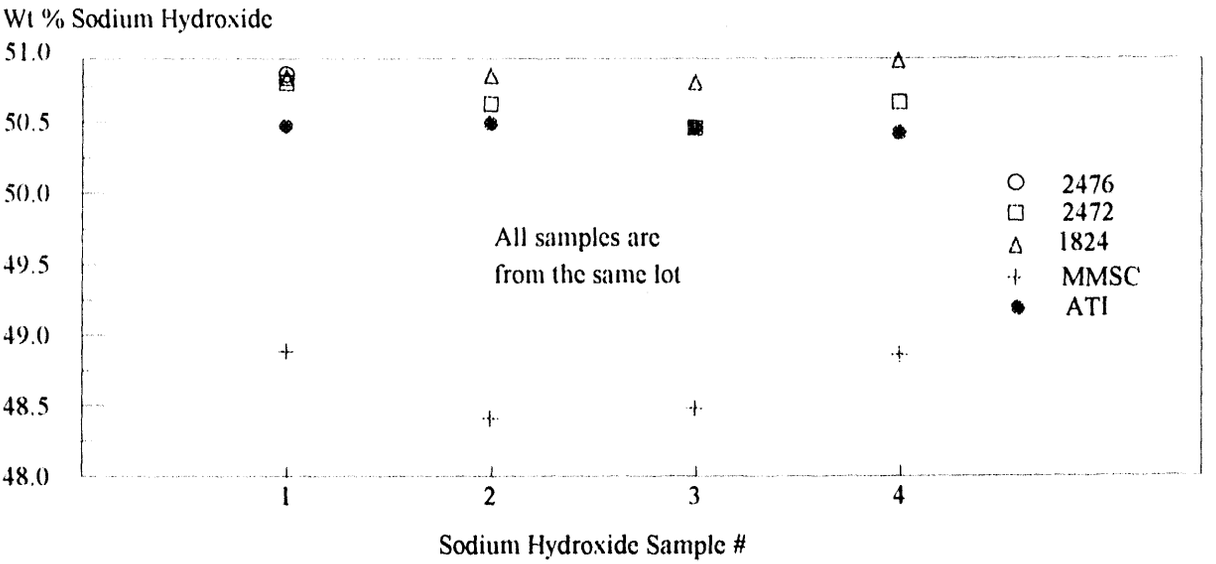

Figure 6. Analytical Round Robin - Sodium Hydroxide Assay

The estimated errors of repeatability for the NaOH assays are presented in Table 7. There is only weak statistical evidence to suggest that the errors of repeatability vary across the different laboratories. The combined estimate of σ_ε is $\hat{\sigma}_\varepsilon = 0.08$.

Table 7. Estimated Std. Dev. of Repeated Measurements (wt%) for NaOH Assays

	2476 (j=1)	2472 (j=2)	1824 (j=3)	ATI (j=4)
$\hat{\sigma}_{\varepsilon_j}$	0.05*	0.10	0.10	0.05

* Note that this estimate is based on four measurements of a single sample.

Table 8 summarizes the systematic differences among the laboratories for the NaOH assays. Again, we will use 2476 (j = 1) as the reference point to compare the estimates of the systematic differences among the laboratories. To assess the statistical significance of these differences we use the methods in the Appendix with $\hat{\sigma}_\gamma = 0.006$ and $\hat{\sigma}_\varepsilon = 0.09$ (obtained using data from 2472, 1824, and ATI assays). Notice that $\hat{\sigma}_\gamma$ is relatively small, yet statistically distinguishable from zero. That $\hat{\sigma}_\gamma$ is statistically different than zero indicates that a component of the assay error is consistent across replicates of the same coded samples. Note that the ATI assays were very consistent across the four coded samples.

Table 8. Systematic Differences Among the Laboratories (wt% NaOH)

	2476 (j=1)	2472 (j=2)	1824 (j=3)	ATI (j=4)
$\hat{C}_j$	----	-0.26	0.02	-0.38

Again, assuming normality and using the methods discussed in the Appendix, we can distinguish systematic differences among the laboratories. These can be represented by:

ATI 2472 2476 1824

Suppose that a sample was submitted to ATI and 1824 (the laboratories providing the most discrepant results for NaOH) for analysis and that each laboratory was to perform n independent assays of that sample. Using the measurement model, the difference between the averages of the $H_2C_2O_4$ assays between the two laboratories, $\overline{Y}_{1824} - \overline{Y}_{ATI}$, is approximately normally distributed with an average of about 0.40 wt% and a standard deviation of about

$\sqrt{2 \cdot (\frac{\hat{\sigma}_\varepsilon^2}{n} + \hat{\sigma}_\gamma^2)}$ (0.13 for n=1). Thus, it is unlikely that individual $H_2C_2O_4$ assays among these five laboratories will exceed one-half to one weight percent.

Two important results were gained from the round robin. One is that several procedural deviations were identified and a more consistent application of the SS drawing procedures was initiated. Secondly, the round robin analysis provided information that was essential in evaluating overall process stability. Note again that we found statistically significant differences among the laboratories with regard to assaying the three compositional materials. Due to the lack of absolute standards (reference materials) we are not able to claim that one laboratory is more or less accurate than another. In some cases we are able to state that one laboratory's assays are more or less precise that those of another. More important than being able to make a direct comparison among laboratories is that we now have an understanding of the magnitude of assay errors. This knowledge was used to help design a mixture experiment in which the goal was to evaluate the effects of compositional variation on the electrical/physical properties of the final product. Together, knowledge of assay uncertainties and the effects of compositional variation led to a fundamental understanding of the robustness of the process with respect to compositional errors introduced by assay variability. Furthermore, as we shall show, the effects of assay variability can be minimized by the proper choice of a target composition.

B. Mixture Experiment

Of the eight compositions in the original design only two (Compositions 1 and 2) did not meet the pH and time processing conditions for an acceptable batch. Composition 1 reached a pH of 6.87 in 180 min, while Composition 2 was terminated at 180 min with a pH of 7.64. Bulk elemental analysis showed that all eight compositions were within specifications for all required elements as well as for all monitored contaminants.

The electrical and physical property data for the wafers prepared from each composition are shown in Table 9. Wafer breakdown field and α are averages of the measurements taken from four electrodes. The standard deviation is shown in parenthesis. Bulk density (calculated theoretical density is 5.57 g/cc) and open porosity were measured by the Archimedes technique in water. It can be seen that of the original eight compositions in the design, only Composition 2 had significantly different electrical properties. There was a less dramatic, but still significant, effect of Composition 2 on bulk density. The radical changes in electrical properties over a relatively small compositional range (from Compositions 1 and 3 to Composition 2) prompted additional experimentation to more clearly define the nature of the changes. Two additional batches were prepared to provide that information. Composition 10 corresponded to the composition of the midpoint of a line segment drawn between Compositions 1 and 3, while Composition 9 corresponded to the midpoint of the line segment drawn between Composition 2 and Composition 10 (see Figure 3). Electrical and physical property data for these compositions are included at the bottom of Table 9.

Table 9. Electrical and Physical Property Results

Comp. #	Breakdown Field (kV/cm) @ 11A/cm^2	α (5-15 A/cm^2)	Bulk Density (g/cc)	%Open Porosity
1	43.24 (0.40)	26.1 (0.9)	5.56	0.0
1	43.04 (0.17)	26.3 (0.7)	5.57	0.0
2	6.85 (0.11)	12.3 (0.8)	5.43	0.0
2	6.81 (0.27)	11.8 (0.5)	5.41	0.0
3	42.91 (0.34)	24.9 (0.8)	5.48	0.0
3	42.90 (0.18)	24.8 (1.0)	5.48	0.0
4	43.57 (0.07)	23.9 (0.8)	5.54	0.0
4	43.52 (0.24)	24.2 (0.7)	5.53	0.0
5	42.32 (0.17)	22.0 (0.2)	5.53	0.1
5	42.23 (0.14)	21.9 (0.4)	5.53	0.2
6	42.77 (0.15)	22.5 (0.4)	5.55	0.0
6	42.72 (0.14)	22.0 (0.4)	5.56	0.0
7	43.91 (0.10)	23.0 (0.1)	5.56	0.1
7	43.81 (0.07)	23.0 (0.1)	5.58	0.0
8 (Run #1)	43.48 (0.20)	24.5 (0.6)	5.53	0.0
8 (Run #1)	43.67 (0.21)	26.1 (0.8)	5.53	0.0
8 (Run #9)	43.42 (0.08)	23.2 (0.3)	5.49	0.0
8 (Run #9)	43.84 (0.14)	23.0 (0.7)	5.49	0.0
9	8.48 (0.08)	14.9 (2.4)	5.50	0.1
9	8.52 (0.15)	14.2 (0.8)	5.49	0.1
10	39.16 (0.26)	17.3 (0.6)	5.51	0.0
10	38.51 (0.48)	17.0 (0.5)	5.50	0.0

The experimental results in Table 9 provide the basis for developing predictive models of the various electrical and physical properties. The predictive models are all of the form

$Y = \beta_0 + \beta_1 \cdot X_1 + \beta_2 \cdot X_2 + \beta_{11} \cdot X_1^2 + \beta_{22} \cdot X_2^2 + \beta_{12} \cdot X_1 \cdot X_2 + \varepsilon$, where

Y is the observed property,

$$X_1 = \frac{1}{.03} \cdot \left\{ \log_e \left(\frac{\text{mole fraction of } ZnCl_2}{\text{mole fraction of NaOH}} \right) + .73 \right\},$$

$$X_2 = \frac{1}{.03} \cdot \left\{ \log_e \left(\frac{\text{mole fraction of } H_2C_2O_4}{\text{mole fraction of NaOH}} \right) + .73 \right\},$$

ε is a measurement error, and the $\beta_{i(j)}$'s are parameters to be estimated. The constants, 0.73 and 0.03, are used to center and scale the logratios so that X_1 and X_2 range approximately between -1 and +1. Note that this centering and scaling process is performed to make computations related to estimating the $\beta_{i(j)}$'s and predicting Y numerically stable.

Use of quadratic response-surface models allows for a great deal of flexibility when modelling data that vary smoothly over the ranges of X_1 and X_2. Because the electrical properties of Compositions 2, 9, and 10 differed radically from the electrical properties of the other compositions, it was not possible to develop a smooth model that has predictive relevance over the entire experimental region. Therefore, the models for electrical properties do not include the data from Compositions 2, 9, or 10 and do not span that compositional region encompassed by them. In the case of bulk density, data from all compositions except Composition 2 were used to develop a predictive model. We were not able to model percent open porosity because of the limited range of the experimental values obtained.

In the case of the breakdown field, the predictive model is given by $Y = \beta_0 + \beta_1 \cdot X_1 + \beta_2 \cdot X_2 + \beta_{11} \cdot X_1^2 + \beta_{12} \cdot X_1 \cdot X_2 + \bar{\varepsilon}$. Estimates of the model parameters, with associated standard errors, are $\hat{\beta}_0$ = 43.6 (0.043), $\hat{\beta}_1$ = -0.419 (0.057), $\hat{\beta}_2$ = 0.347 (0.051), $\hat{\beta}_{11}$ = -0.626 (0.047), and $\hat{\beta}_{12}$ = 0.398 (0.052). The estimated standard deviation of the measurement error averaged over the four electrodes ($\bar{\varepsilon}$) is $\hat{\sigma}_{\bar{\varepsilon}}$ = 0.12. This is reasonably consistent with the standard deviations of the measurements of the electrodes within each run. Thus, the magnitude of the differences between the observed data and the model is largely a consequence of measurement error and variability from electrode to electrode.

Figure 7 is a contour plot of the breakdown field model. The shaded region is that area of the design space that could not be modelled due to the significantly lower breakdown field value for Composition 2. The average breakdown field for Compositions 2, 9, and 10 are shown on the plot. Looking at the modelled area reveals that the entire region is relatively flat with a slight upward slope toward the left edge of design space. The model matches the experimental data quite well as typical deviations of the experimental data from the model are about 0.1 kV/cm. Most importantly, typical breakdown fields are centered within the breakdown field specification of 43.0 ± 2.0 kV/cm. Unfortunately, the nominal composition is not well centered on this region and in fact variation, from the target, introduced by assay errors could generate compositions in the region where the breakdown field begins its precipitous drop.

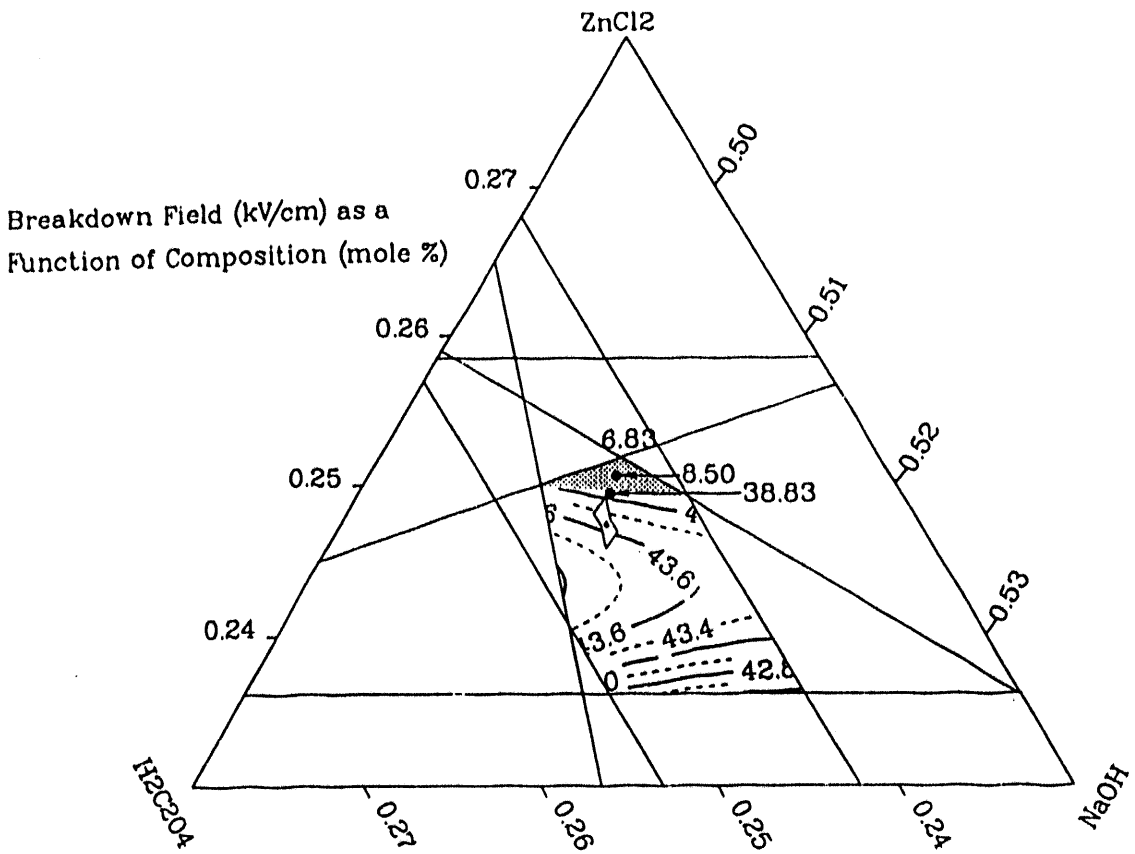

Figure 7. Breakdown Field Model

The model for breakdown field provides a possible explanation for some failed producibility batches at MMSC in 1991. Several batches prepared at MMSC had breakdown field values <10 kV/cm, but appeared to have been processed correctly. These batches also showed that all elements were present in the bulk within specifications and that all contaminant levels were acceptable. The assay "errors" required to generate the Compositions 9 and 10 are given in Table 10. For $ZnCl_2$ and NaOH those "errors" for both compositions are well within the assay uncertainties observed in the round robin. The $H_2C_2O_4$ "error" is somewhat larger than what would be expected from the round robin study. However, we feel the process could have been made unstable through certain combinations of relatively small assaying and/or weighing errors.

Table 10. Assay "Errors" Corresponding to Compositions 9 and 10

	Zinc Chloride		Oxalic Acid		Sodium Hydroxide	
Comp. #	Mole Fraction	Assay "Error" (wt%)	Mole Fraction	Assay "Error" (wt%)	Mole Fraction	Assay "Error" (wt%)
9	0.2508	-0.59	0.2453	0.91	0.5040	0.10
10	0.2495	-0.36	0.2463	0.49	0.5045	0.05

In the case of α, the predictive model is given by $Y = \beta_0 + \beta_1 \cdot X_1 + \beta_2 \cdot X_2 + \beta_{22} \cdot X_2^2 + \beta_{12} \cdot X_1 \cdot X_2 + \bar{\varepsilon}$. Note that results from run #9, with regard to α appear to be discrepant with the remaining body of data. Therefore, data from run #9 were not used to estimate the model parameters. Estimates of the model parameters, with associated standard errors, are $\hat{\beta}_0$ = 25.5 (0.30), $\hat{\beta}_1$ = 0.964 (0.21), $\hat{\beta}_2$ = 0.558 (0.32), $\hat{\beta}_{22}$ = -1.53 (0.45), and $\hat{\beta}_{12}$ = 0.761 (0.24). The estimated standard deviation of the measurement error averaged over the four electrodes ($\bar{\varepsilon}$) is $\hat{\sigma}_{\varepsilon}$ = 0.52. Again, this is reasonably consistent with the standard deviations of the measurements of the electrodes within each run.

Figure 8 displays the model for α. Except for the area approaching Composition 2, the modelled region is within specification (α>15) and has a relatively flat surface that slopes up slightly at the contour cliff. The risk of batch failure utilizing the nominal composition is not as likely as with breakdown field. Composition 10 meets the α specification and therefore normal assaying errors should not generate compositions that would yield unacceptable product with respect to α.

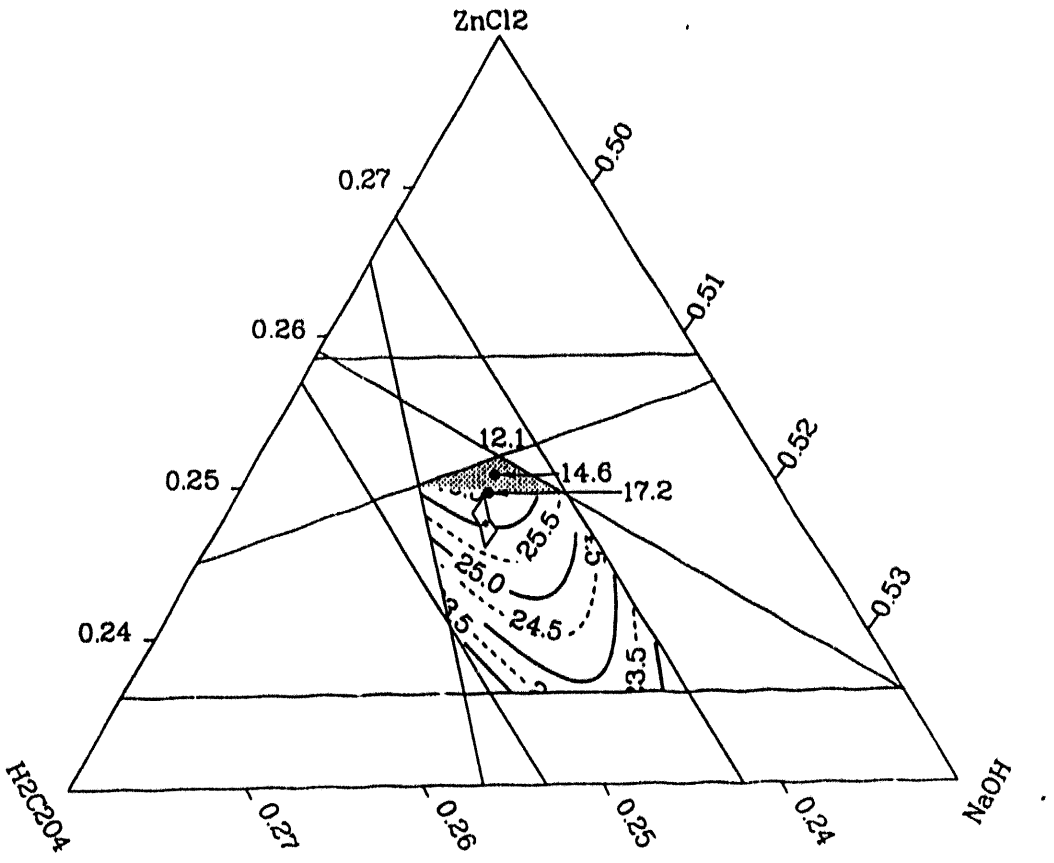

Figure 8. α Model

In the case of the bulk density, the predictive model is given by $Y = \beta_0 + \beta_1 \cdot X_1 + \beta_2 \cdot X_2 + \beta_{11} \cdot X_1^2 + \beta_{12} \cdot X_1 \cdot X_2 + \bar{\varepsilon}$. Again, the results from run #9, with regard to bulk density appear to be discrepant with the remaining body of data. Therefore, data from run #9 were not used to estimate the model parameters. Estimates of the model parameters, with associated standard errors, are $\hat{\beta}_0$ = 5.52 (0.0042), $\hat{\beta}_1$ = -0.0318 (0.0038), $\hat{\beta}_2$ = 0.0434 (0.0043), $\hat{\beta}_{11}$ = -0.0158 (0.0039), and $\hat{\beta}_{12}$ = 0.0251 (0.0043). The estimated standard deviation of the measurement error averaged over the four electrodes ($\bar{\varepsilon}$) is $\hat{\sigma}_{\bar{\varepsilon}}$ = 0.01. Again, this is reasonably consistent with the standard deviations of the measurements of the electrodes within each run.

Figure 9 displays the model for bulk density. All compositions are still well within product specifications (95% of theoretical corresponds to 5.29 g/cc). Thus, it is highly unlikely that assay errors would have a practical effect on bulk density.

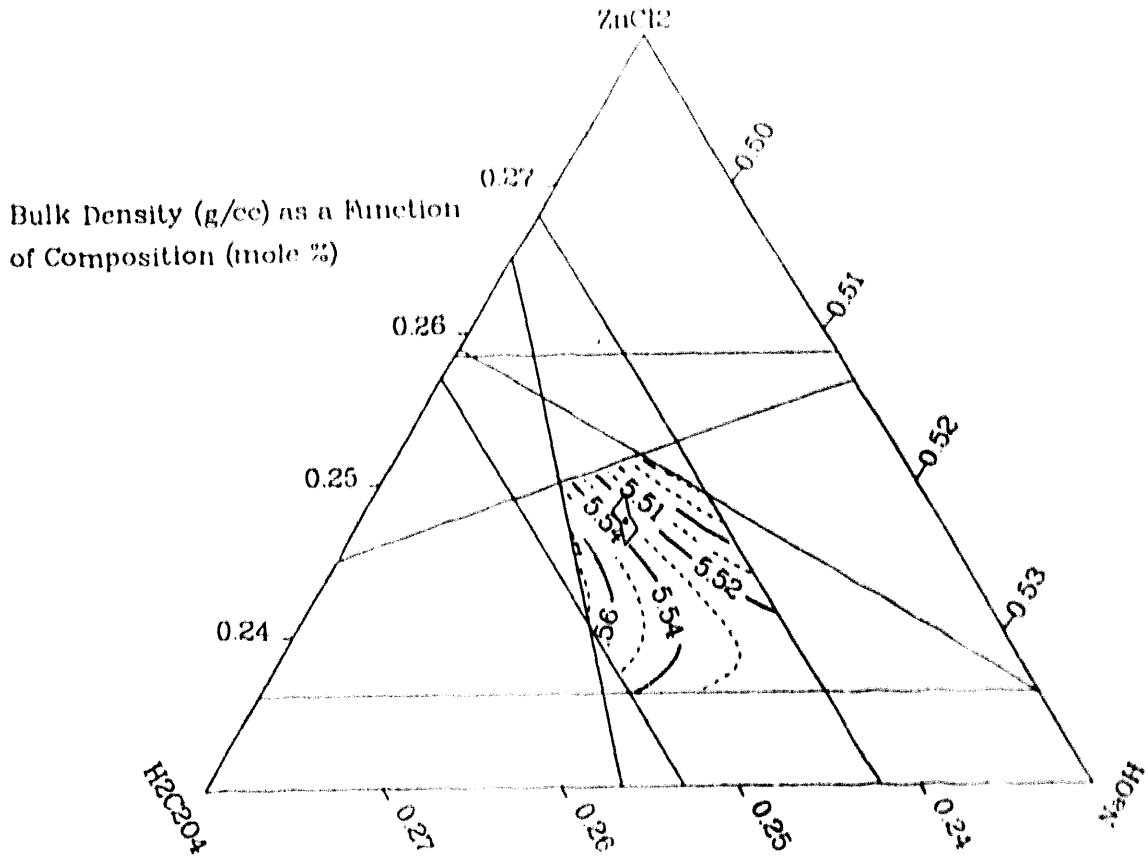

Figure 9. Bulk Density Model

Based upon the data and subsequent analysis from the mixture experiment, the obvious recommendation is to move the nominal composition to the center of the modelled region. This would reduce the consequences of compositional variation due to assay errors on product quality. This would even allow the use of manufacturer's assay values for the $H_2C_2O_4$ and the NaOH, thus saving the expense and time of assaying those two reagents (the $ZnCl_2$ solution is prepared from a powder and would still require assaying).

All previous work on the chem-prep process has indicated that wafer properties accurately predict rod component properties. However, to confirm that moving the composition would be "transparent", 20 rods were made from the center point composition and put through the standard 25 pulse screening test (reference may be requested from the authors). The survival rate of 75% was within the same range seen for rods prepared from the original composition. Testing of the rods at the next assembly level is not scheduled at this time due to funding limitations.

C. Analysis of Failed Batches

The mixture experiment also revealed that the solution chemistry was more complex and not as well understood as originally thought. As stated earlier, one of the assumptions upon

which the constraints were based was that the slurry had to rapidly enter a basic regime to quantitatively and homogeneously precipitate all metal species (particularly Al^{3+}). However, Composition 1 had a final pH below 7.0 (the specification requires achievement of pH of 8.0 within 150 min), but met all electrical and physical specifications. Composition 2 which also failed to reach pH 8.0 had very poor electrical properties despite having the specified bulk elemental distribution.

To investigate this situation further, SEM photographs of a Composition 2 wafer and a nominal composition wafer were taken (see Figure 10). The reason for the low breakdown field in Composition 2 is readily apparent. Since the breakdown field is proportional to the number of grain boundaries per given length, the large grains observed in the Composition 2 wafer account for the lower breakdown field. It is well documented that low levels of Al^{3+} will inhibit grain growth in ZnO-based varistors.[2,6-7] The minimum level of Al^{3+} needed to preserve sub-micron grain size for high field material has been determined to be 100 ppm.[2] Since Composition 2 had 130 ppm Al^{3+}, it appears that the Al^{3+} distribution is the problem. The bimodal distribution of sub-micron and 5-10 micron sized grains strongly suggests an inhomogenous distribution of the Al^{3+}. Unfortunately, the levels of Al^{3+} were too low to confirm the Al^{3+} distribution by microprobe or TEM analyses. ICP-AES analysis of the oxalate samples taken at various time intervals showed that even at 0 time (actually it was 5-10 min after oxalate addition before the sample was completely processed) the Al^{3+} level in Composition 2 was 130 ppm. Clearly the critical kinetics are occurring very rapidly and a special experimental set-up will be required to correlate the Al^{3+} precipitation kinetics with distribution.

Composition 1 had an even poorer pH response yet there does not appear to be any Al^{3+} distribution effects in that batch. However, Composition 1 had excess oxalic acid. Al^{3+} hydrolysis calculations show that Al^{3+} solubility decreases with increasing oxalate concentration. Determining whether the relatively small excess oxalic acid concentration in Composition 1 was able to suppress the Al^{3+} solubility sufficiently for homogenous distribution will require additional investigation. Nevertheless, control of Al^{3+} solution chemistry in this system is clearly more complex than simply adjusting the pH. Additional experiments will be required to unravel the interactions of pH and oxalate solubility.

Nominal Composition

Composition 2

Figure IV. SEM Comparison: Composition 2 with Nominal Composition Material

IV. Conclusions:

The stability of the chemistry process with respect to assayed errors was investigated. A round robin study among the laboratories was conducted to determine the variability of assays both among and within the laboratories. The study was used in the identification and correction of several procedural deviations.

The quantification of assay variability among and within laboratories was used to design a mixture experiment comprised of ZrO_2, $H_2C_2O_4$, and NaOH. Based on the experimental data from the mixture experiment, models of breakdown field, σ, and bulk density were constructed. The models showed that there was a very large compositional region where all electrical and physical property specifications were met, but that the nominal composition was situated on the edge of this region. It appears that normal assayed errors in combination with relatively small process variations could generate unacceptable product. As a result, the target composition was moved to the center of the compositional region that met all electrical and physical property specifications. Not only did this improve process stability, but it allowed for the use of the manufacturer's assays and therefore eliminated the need to reassay two of the three components. Rods fabricated from wafers of the center point composition performed comparably to rods fabricated from the nominal composition.

V. Appendix:

Statistical Procedures Used in the Analysis of Round Robin Results

The purpose of this appendix is to give the computational formulae and procedures used to analyze the round robin results. The procedures given here can be used for arbitrary l, m, and n, where,

l = number of samples analyzed,

m = number of labs, and

n = number of replicates per la per sample.

The procedures that follow are valid in the case of balanced data (i.e., the number of replicates is constant for each sample/lab combination). For analysis of unbalanced data see Reference 8.

To aid this presentation, the following notation will be used. First, recall that Y_{ijk} = the analytical determination of the k^{th} replicate by the j^{th} lab for the i^{th} sample.

$$\overline{Y}_{ij} = \frac{1}{n} \cdot \sum_{k=1}^{n} Y_{ijk}$$

$$\overline{Y}_{i} = \frac{1}{m \cdot n} \cdot \sum_{j=1}^{m} \sum_{k=1}^{n} Y_{ijk}$$

$$\overline{Y}_{j} = \frac{1}{l \cdot n} \cdot \sum_{i=1}^{l} \sum_{k=1}^{n} Y_{ijk}$$

$$\overline{Y} = \frac{1}{l \cdot m \cdot n} \cdot \sum_{i=1}^{l} \sum_{j=1}^{m} \sum_{k=1}^{n} Y_{ijk}$$

These averages can be used to form the following summary statistics which partition the observed variability of Y_{ijk}.

$$MS_{samples} = \frac{m \cdot n}{l-1} \cdot \sum_{i=1}^{l} (\overline{Y}_{i} - \overline{Y})^2$$

$$MS_{labs} = \frac{l \cdot n}{m-1} \cdot \sum_{j=1}^{m} (\overline{Y}_{j} - \overline{Y})^2$$

$$MS_{labs \times samples} = \frac{n}{(l-1)(m-1)} \cdot \sum_{i=1}^{l} \sum_{j=1}^{m} (\overline{Y}_{ij} - \overline{Y}_{i} - \overline{Y}_{j} - \overline{Y})^2$$

$$MS_{error} = \frac{1}{l \cdot m \cdot (n-1)} \cdot \sum_{i=1}^{l} \sum_{j=1}^{m} \sum_{k=1}^{n} (Y_{ijk} - \overline{Y}_{ij})^2$$

Finally, these summary statistics are used to estimate the model parameters that are presented in Section III.A of this report. First, we will consider the measurement error associated with repeatability (ε). If the magnitude of the repeatability error is similar across labs, then a pooled estimate of σ_ε is

$$\hat{\sigma}_\varepsilon = \sqrt{\text{MS}_{\text{error}}}.$$

Lab-specific estimates of σ_ε are

$$\hat{\sigma}_{\varepsilon_j} = \sqrt{\frac{1}{l\cdot(n-1)}\cdot\sum_{i=1}^{l}\sum_{k=1}^{n}(Y_{ijk}-\overline{Y}_{ij})^2}\text{, for j = 1,2,..., m.}$$

Next, an estimate of $\hat{\sigma}_\gamma$ is

$$\hat{\sigma}_\gamma = \sqrt{\frac{\text{MS}_{\text{labs x samples}} - \text{MS}_{\text{error}}}{n}}.$$

An estimate of the contrast between two labs indexed by j′ and j is

$$C(j',j) = \overline{Y}_{j'} - \overline{Y}_{j}.$$

The estimated standard deviation of the random uncertainty in the statistic C(j′,j) is

$$\hat{\sigma}_{C(j',j)} = \sqrt{\frac{2\cdot\hat{\sigma}_\gamma^2}{l} + \frac{\hat{\sigma}_{\varepsilon_{j'}}^2}{l\cdot n} + \frac{\hat{\sigma}_{\varepsilon_j}^2}{l\cdot n}},$$

or, in the case where the magnitude of the repeatability error is similar across labs,

$$\hat{\sigma}_{C(j',j)} = \sqrt{\frac{2\cdot\hat{\sigma}_\gamma^2}{l} + \frac{\hat{\sigma}_\varepsilon^2}{l\cdot n}}.$$

The degrees of freedom associated with $\hat{\sigma}_{C(j',j)}$ are $(l\text{-}1)\cdot(m\text{-}1)$.

The assessment of whether or not the labs produce statistically different assays is as follows. First, an F-test is performed to see if the C(j′,j)'s, collectively for all combinations of j′ and j, are statistically different than zero. Second, if it is determined from the F-test that there are significant differences among the C(j′,j)'s , t-tests can be performed to assess the statistical significance of differences between two specific labs. The F-statistics are constructed as

$$F = \frac{\text{MS}_{\text{labs}}}{\text{MS}_{\text{labs x samples}}}.$$

If $F > \mathcal{F}_{1-\alpha;(m-1),(l-1)\cdot(m-1)}$, where $\mathcal{F}_{1-\alpha;(m-1),(l-1)\cdot(m-1)}$ is the 1-α percentile of the $\mathcal{F}$-distribution with m-1 and (l-1)·(m-1) degrees of freedom, then we conclude that there are some significant differences among the labs. The level of the test, α,refers to the probability of falsely concluding that there are significant differences when in fact there are not. for purposes of evaluating the various F-statistics (and t-statistics) we use $\alpha = 0.05$.

The t-statistics, relevant for comparing the j'th and jth labs are computed as

$$t = \frac{C(j', j)}{\hat{\sigma}_{C(j',j)}}$$

if $|t| > T_{1-\frac{\alpha}{2};(m-1)}$, where $T_{1-\frac{\alpha}{2};(m-1)}$ is the 1-$\frac{\alpha}{2}$ percentile of the T-distribution with m-1 degrees of freedom, then we conclude that the j'th lab produces significantly different assays than the jth lab. Also, the sign of t indicates whether assays from the j'th lab were higher or lower than assays from the jth lab.

Note that by interpreting the F- and t-statistics probablistically, we are implicitly assuming that the ε_{ijk} and the γ_{ij} terms are normally distributed.

VI. References

1. R. G. Dosch and K. M. Kimball, *Chemical Preparation of High-Field Zinc Oxide Varistors*, SAND85-0195. Sandia National Laboratories, Albuquerque, NM, September, 1985.

2. K. M. Kimball and D. H. Doughty, *Aluminum Doping Studies on High Field ZnO Varistors*, SAND86-0713. Sandia National Laboratories, Albuquerque, NM, August, 1987.

3. T. J. Gardner, D. H. Doughty, S. J. Lockwood, B. A. Tuttle, and J. A. Voigt, the Effect of Low Level Dopants on Chemically Prepared Varistor Materials, in *Transactions in Ceramics - Proceedings of the Second International Varistor Conference*, held in Schenectady, NY, December, 1988, American Ceramics Society.

4. S. J. Lockwood and T. J. Gardner, *Washing and Filtration Study of the 1 kg Batch-Type Chemical Powder Preparation Process for High Field Varistor Fabrication*, SAND87-2180. Sandia National Laboratories, Albuquerque, NM, June, 1988.

5. T. J. Gardner and S. J. Lockwood, *Sintering Schedule and Sample Geometry Effects on the Electrical and Physical Properties of High Field Varistor Materials*, SAND88-2449. Sandia National Laboratories, Albuquerque, NM, February, 1989.

6. W. G. Carlson and T. K. Gupta, Improved Varistor Nonlinearity Via Donor Impurity Doping, in *J. Appl. Phys.*, vol. 53, no. 8, pp. 5746-53, 1982.

7 Tsai, C. L. Huang, and C. C. Wei, Improvement of Nonlinearity in a ZnO Varistor by Al_2O_3 Doping, in J. Mat. Sci. Letters, vol. 4, pp. 1305-7, 1985.

8. Searle, S. R., Casella, G., and McCulloch, C. E., *Variance Components*, John Wiley, New York, 1992.

Distribution

0300 R. L. Schwoebel
0323 R. G. Easterling
0323 E. V. Thomas (5)
1846 W. F. Hammetter, actg.
1846 J. A. Voigt
2400 J. Q. Searcy
2402 J. L. Ledman
2476 F. P. Gerstle, Jr.
2476 S. C. Douglas
2476 T. J. Gardner
2476 S. J. Lockwood (5)
2523 D. H. Doughty
2565 P. J. Wilson
2565 T. W. Scofield

Martin Marietta Specialty Components
P.O. Box 2908
Largo, FL 34294
S. DeNino

Alliant Techsystems, Inc.
5121 Winnetka Ave. North
New Hope, MN 55428
F. Wallenhorst

7141 Technical Library (5)
7151 Technical Publications
7613-2 Document Processing for DOE/OSTI (10)
8523-2 Central Technical Files

DATE
FILMED
11/8/93
END